Semaphorin SEMA3F Affects Multiple Signaling Pathways in Lung Cancer Cells

Vincent A. Potiron,[1,2] Girish Sharma,[1] Patrick Nasarre,[3,4] Jonathan A. Clarhaut,[2] Hellmut G. Augustin,[3,4] Robert M. Gemmill,[1] Joëlle Roche,[2] and Harry A. Drabkin[1]

[1]Division of Medical Oncology, University of Colorado Health Sciences Center, Aurora, Colorado; [2]CNRS UMR 6187, Institut de Physiologie et Biologie Cellulaires, Faculté des Sciences de Poitiers, Poitiers, France; [3]Department of Vascular Biology and Angiogenesis Research, Tumor Biology Center, Freiburg, Germany; and [4]Joint Research Division Vascular Biology, Medical Faculty Mannheim, University of Heidelberg and German Cancer Research Center, Heidelberg, Germany

Abstract

Loss of SEMA3F occurs frequently in lung cancer and correlates with advanced stage of disease. We previously reported that SEMA3F blocked tumor formation by H157 lung cancer cells in a rat orthotopic model. This was associated with loss of activated $\alpha_V\beta_3$ integrin, impaired cell adhesion to extracellular matrix components, and down-regulation of phospho-extracellular signal-regulated kinase 1/2 (ERK1/2). These results suggested that SEMA3F might interfere with integrin outside-in signaling. In the present report, we found that SEMA3F decreased adhesion to vitronectin, whereas integrin-linked kinase (ILK) kinase activity was down-regulated in SEMA3F-expressing H157 cells. Exposure to SEMA3F-conditioned medium led to diminution of phospho-ERK1/2 in four of eight lung cancer cell lines, and ILK silencing by small interfering RNA led to similar loss of phospho-ERK1/2 in H157 cells. Moreover, SEMA3F expression (with constitutive and inducible systems) also reduced AKT and signal transducer and activator of transcription 3 (STAT3) phosphorylation independently of ILK-ERK1/2. These signaling changes extended downstream to hypoxia-inducible factor-1α (HIF-1α) protein and vascular endothelial growth factor (VEGF) mRNA levels, which were both reduced in three of four *SEMA3F*-transfected cell lines. Mechanistically, the effects on HIF-1α were consistent with inhibition of its AKT-driven protein translation initiation, with no effect on HIF-1α mRNA level or protein degradation. Furthermore, when H157 cells were injected s.c. in nude mice, tumors derived from SEMA3F-expressing cells showed lower microvessel density and tumor growth. These results show that SEMA3F negatively affects ILK-ERK1/2 and AKT-STAT3 signaling, along with inhibition of HIF-1α and VEGF. These changes would be anticipated to contribute significantly to the observed antitumor activity of SEMA3F. [Cancer Res 2007;67(18):8708–15]

Introduction

The semaphorin *SEMA3F* gene was originally cloned from a recurrent homozygous deletion involving chromosomal region 3p21.3 (1–3). SEMA3F is abundantly expressed in normal lung and cultured bronchial epithelial cells. In contrast, it is markedly down-regulated in most human lung cancers and loss of SEMA3F protein staining is significantly correlated with advanced stage of disease and vascular endothelial growth factor-165 ($VEGF_{165}$) overexpression (4, 5). We previously reported that retroviral-mediated replacement of SEMA3F expression blocked tumor formation by H157 lung cancer cells when injected into the lungs of immunodeficient rats. This was associated with loss of activated $\alpha_V\beta_3$ integrin, impaired cell adhesion to extracellular matrix (ECM), and down-regulation of phospho-extracellular signal-regulated kinase 1/2 (ERK1/2; ref. 6).

Class 3 semaphorins, including SEMA3F, are secreted proteins originally identified as mediators of growth cone repulsion (7). With the exception of SEMA3E, class 3 semaphorins use high-affinity neuropilin (NRP) 1 and NRP2 receptors and plexin coreceptors to mediate their biological activities (see ref. 8 for review). NRP1 was also independently identified as a coreceptor for $VEGF_{165}$ and placenta growth factor-2 (9, 10), and a subset of class 3 semaphorins has been shown to competitively inhibit $VEGF_{165}$ binding and function (11, 12). In addition to their effects on Rac activation (13, 14), class 3 semaphorins regulate integrin function (15, 16). This can be explained by the GTPase-activating protein activity of plexins for R-Ras (17, 18) and sequestration of talin by PIPKI-γ661 (14). Integrins, composed of transmembrane α and β heterodimers, bind ECM components and signal in a bidirectional manner (19). This suggested to us that integrin-linked kinase (ILK), which interacts with β-integrins and has multiple protumorigenic activities including AKT phosphorylation (20, 21), might be affected by SEMA3F. In the present report, we found that ILK activity was inhibited by SEMA3F in H157 lung cancer cells, along with down-regulation of adhesion to vitronectin. Exposure to SEMA3F, or inhibition of ILK by small interfering RNA (siRNA), led to decreased ERK1/2 signaling, which was observed in different lung cancer cell lines. Moreover, SEMA3F reduced AKT and signal transducer and activator of transcription 3 (STAT3) phosphorylation in H157 cells in a manner that was independent of ILK but consistent with Src inhibition. These changes were accompanied by downstream loss of hypoxia-inducible factor-1α (HIF-1α) protein and decreased VEGF mRNA levels in three of four *SEMA3F* stably transfected cell lines. Lastly, we show that these effects were mirrored by reductions in microvessel density and tumor growth following s.c. implantation of SEMA3F-expressing H157 cells in nude mice. These results show that SEMA3F inhibits diverse signaling pathways in responsive lung cancer cells, possibly contributing to its observed antitumor activity.

Materials and Methods

Cell lines and animals. All cultures were grown in regular RPMI 1640 supplemented with 10% FCS and appropriate selection drugs.

Note: Supplementary data for this article are available at Cancer Research Online (http://cancerres.aacrjournals.org/).

G. Sharma and P. Nasarre contributed equally to this work.

Requests for reprints: Harry A. Drabkin, Division of Hematology/Oncology, Medical University of South Carolina, P. O. Box 250623, 96 Jonathan Lucas Street, Charleston, SC 29425. Phone: 843-792-8297; E-mail: drabkin@musc.edu.

doi:10.1158/0008-5472.CAN-06-3612

Establishment and maintenance of NCI-H157 and NCI-H460 (hereafter H157 and H460) lung cancer cells stably transfected by retrovirus with *SEMA3F* has been described previously (6). Briefly, myc-tagged *SEMA3F* was cloned into pLXSN retroviral vector and cells were infected using retrovirus-containing culture medium from PT67 packaging cells. Stable SEMA3F (or empty vector)-expressing MCF7 and COS7 cell populations were obtained by retroviral transfection as described above and in ref. 6. Cells were selected and grown with 500 μg/mL G418 (Invitrogen). Establishment of H157 cells with stably integrated *SEMA3F* under the control of a tetracycline-inducible promoter was obtained following the Flp-In T-REx Core kit instructions (Invitrogen) after cloning 3′ myc-tagged *SEMA3F* in pcDNA5/FRT/TO (Invitrogen) at *Eco*RV site. Empty vector–transfected ("inducible H157EV") and *SEMA3F*-transfected ("inducible H157S3F") cell populations were selected and grown with 100 μg/mL hygromycin and 5 μg/mL blasticidin (Invitrogen). SEMA3F was induced for 5 days with doxycycline at 5 or 100 ng/mL. Microsatellite genotyping was done by the UC Cancer Center DNA Sequencing Core to confirm authenticity of cells. Supplementary information is available on SEMA3F mRNA expression and related transcripts (Supplementary Table S1). All animal experiments followed the guidelines of the Animal Committee of the Regienrungsprasidium Freiburg (Germany).

Proteins and reagents. Recombinant proteins were purchased from Chemicon International (Millipore), except VEGF and vitronectin (R&D Systems). LY294002, cobalt chloride ($CoCl_2$), and cycloheximide were from Sigma-Aldrich. PP2 and PP3 were from Calbiochem. UO126 was from Promega and doxycycline was from Sigma-Aldrich. SEMA3F-conditioned media were prepared as follows: 1×10^6 H157S2 cells were plated in a 100-mm dish with 4 mL RPMI 1640 + 10% FCS. After 24 h of culture, media were collected and centrifuged briefly to eliminate cell residue. H157C-conditioned medium was used as a control.

RNA expression. Total RNA was extracted using the RNeasy Mini kit (Qiagen). Reverse transcription-PCR (RT-PCR) was done with SuperScript III (Invitrogen) using the procedure supplied by the manufacturer. Gene expression was assessed relative to glyceraldehyde-3-phosphate dehydrogenase (GAPDH) by quantitative real-time PCR with the GeneAmp 5700 Sequence Detection System and SYBR Green chemistry (Applied Biosystems; ref. 6). Primer sequences were as follows: GAPDH, 5′-TGCACCACCAACTGCTTAGC-3′ and 5′-GGCATGGACTGTGGTCATGAG-3′; HIF-1α, 5′-CATTACCCACCGCTGAAACG-3′ and 5′-TTCACTGGGACTATTAGGCTC-3′; and VEGF, 5′-CAAGACAAGAAAATCCCTGTGG-3′ and 5′-CCTCGGCTTGTCACATCTG-3′.

siRNA transfection. ILK and related scramble siRNAs were purchased from Ambion and transfected using LipofectAMINE 2000 as recommended (Invitrogen).

Immunoblotting. Immunoblots were done as reported (6). The primary antibodies rabbit anti-AKT, anti–phospho-Ser^{473}-AKT, anti-STAT3, anti–phospho-Tyr^{705}-STAT3, and anti–phospho-Thr^{202}/Tyr^{204}-ERK1/2 were from Cell Signaling Technology and used at 1:1,000 dilution. Anti-ERK1/2 (1:4,000) and phospho-Tyr^{397}-focal adhesion kinase (FAK; 1:1,000) were from Promega and Chemicon, respectively. Anti-HIF-1α (1:300) and anti–phospho-serine/threonine (1:1,000) were from Transduction Laboratories. Anti-ILK (1:1,000) was from Upstate Biotechnology. Antiactin and antitubulin were from Sigma-Aldrich (1:2,000). Horseradish peroxidase (HRP)-conjugated antimouse and antirabbit secondary antibodies (Perkin-Elmer) were used at 1:5,000 dilution. Detection was done with enhanced chemiluminescence (Perkin-Elmer).

Immunoprecipitation and kinase assay for ILK. Ten million cells were lysed in 500 μL of lysis buffer [50 mmol/L HEPES (pH 7.4), 100 mmol/L NaCl, 1.5 mmol/L $MgCl_2$, 0.5% CHAPSO, 1 mmol/L NaF and Na_3VO_4, 5 μg/mL leupeptin and aprotinin, 1 μg/mL pepstatin A]. Protein (500 μg) was precleared by incubation with 50 μL protein G-agarose beads (Roche) and then centrifuged for 5 min at 900 rpm. The supernatant was incubated overnight at 4°C with 5 μg of anti-ILK. Protein G-agarose beads were added for 3 h and immune complexes were pelleted for 1 min at 3,000 rpm. Pellets were washed thrice in lysis buffer and resuspended in 100 μL of kinase assay buffer [50 mmol/L HEPES (pH 7.4), 2 mmol/L each of $MnCl_2$, $MgCl_2$, Na_3VO_4, and NaF]. In parallel, purity of the immunoprecipitate was checked by total protein staining using Silver Stain Plus (Bio-Rad). The kinase reaction was done by adding 2 μL of 10 mmol/L ATP and 2 μg of myelin basic protein (MBP; Upstate Biotechnology) to 50 μL of ILK immunoprecipitate resuspended in kinase assay buffer. The reaction was incubated for 30 min at 30°C and stopped by denaturing samples at 100°C in Laemmli electrophoresis loading buffer.

Immunofluorescence. Cells grown on glass coverslips were fixed for 15 min with 3.7% formalin. After rinsing with PBS, primary and secondary antibodies were each applied for 90 min at room temperature and then rinsed. Anti–HIF-1α was used at 1:100 dilution. Activated $\alpha_v\beta_3$ integrin was detected as described (6). Alexa^{488}-conjugated antirat and Alexa^{564}-conjugated antirabbit secondary antibodies (1:250) were from Molecular Probes. Stained slides were rinsed in PBS and mounted in Vectashield (Vector Laboratories), and images were captured with a confocal microscope (Olympus FluoView FV1000) at 100× immersion oil objective.

Adhesion assay. One thousand untransfected H157 cells in 100 μL of fresh medium were mixed to 100 μL of SEMA3F or control-conditioned medium and deposited on vitronectin-coated (0.5 μg/mL) wells. Cells were allowed to attach for 1 h and processed as detailed previously (6).

VEGF ELISA. Human VEGF dosage on culture supernatants was done following the manufacturer's instructions (R&D Systems).

Tumor xenograft experiments. Female athymic nude mice (NMRI-*nu/nu*) were purchased from Charles River Laboratories. S.c. injection of 2.5×10^5 cells in Matrigel was done into the right flanks using a 29-gauge needle syringe. Tumor volume (mm^3) was calculated by caliper measurements of the largest diameter (a) and its perpendicular (b) according to the following formula: volume = $0.5ab^2$.

Immunohistochemistry and microvessel density quantification. Cryosections (8 μm), fixed with 4% paraformaldehyde, were stained for mouse CD31 using a rat primary antibody (1:100; BD PharMingen) and Alexa^{488}-conjugated antirat secondary antibody (1:200). Slices were counterstained with 4′,6-diamidino-2-phenylindole and microvessel density was determined by counting the number of CD31$^+$ blood vessels using the program Cell-P (Olympus).

Results

Inhibition of ERK1/2, AKT, and STAT3 by SEMA3F. Previously, we reported that inhibition of *in vivo* tumor formation by SEMA3F is associated with decreased ERK1/2 activation (6). To extend these investigations, we asked if alternative signaling pathways might also be affected by SEMA3F. For this, we first used the H157 lung cancer cell line that has been previously modified by retrovirus-mediated transfection to constitutively reexpress SEMA3F (6). One control and two independent SEMA3F (S1 and S2) clones were selected. Expression of SEMA3F was verified at the mRNA and protein levels, and secretion of SEMA3F was shown by immunoblot analysis of culture medium (see Supplementary Fig. S1*A* and Supplementary Table S1). At the mRNA level, SEMA3F expression was approximately 2-fold (clone S1) to 8-fold (clone S2) greater than detected in normal lung, and there was no significant clonal variations (6). As shown in Fig. 1*A*, we found that phospho-AKT (Ser^{473}) and phospho-STAT3 (Tyr^{705}) were down-regulated in *SEMA3F* stably transfected H157 cells (H157S2) compared with controls (H157C). Similar results were also observed in the independent SEMA3F-expressing clone, H157S1 (data not shown). Furthermore, the addition of exogenous growth factors did not reverse the SEMA3F effects on phospho-AKT and phospho-STAT3. In contrast, stimulation with growth factors was able to overcome the inhibition of phospho-ERK1/2 (Fig. 1*A*).

To confirm the effects on AKT-STAT3, we generated stable isogenic H157 control (empty vector) and SEMA3F cells in which

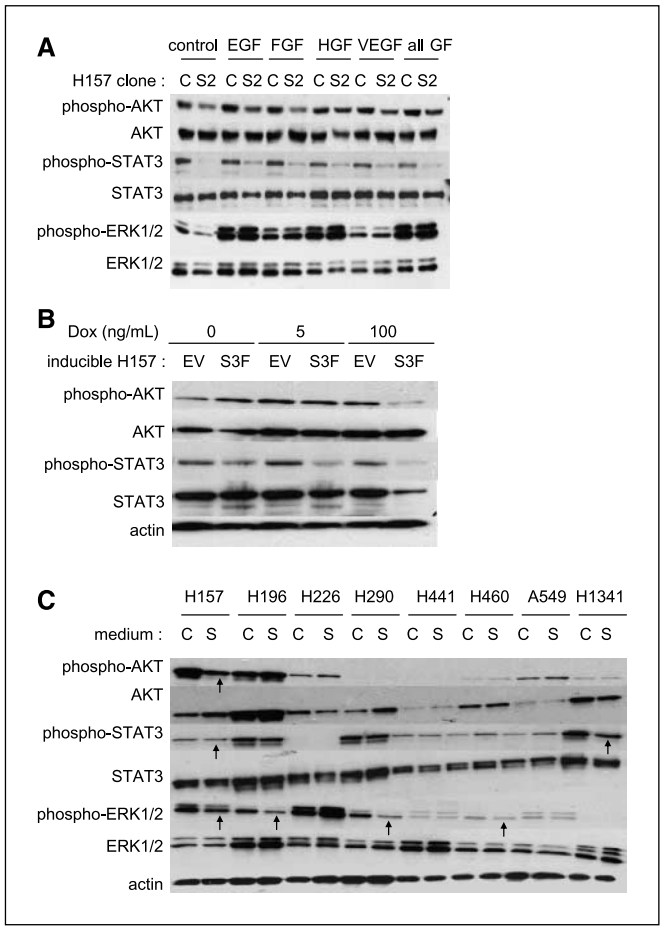

Figure 1. SEMA3F inhibits multiple signaling pathways in lung cancer cell lines. *A,* H157C (*C*) and H157S2 (*S2*) clones were stimulated for 15 min with 100 ng/mL of the indicated growth factors. Protein extracts were subjected to immunoblot for phospho-Ser^{473}-AKT and total AKT, phospho-Tyr^{705}-STAT3 and total STAT3, and phospho-Thr^{202}/Tyr^{204}-ERK1/2 and total ERK1/2. *EGF,* epidermal growth factor; *FGF,* fibroblast growth factor; *HGF,* hepatocyte growth factor; *GF,* growth factor. *B,* H157EV (*EV*) and H157S3F (*S3F*) cells were induced with doxycycline (*Dox*) for 5 d and immunoblots were done as in *A. C,* indicated lung cancer cell lines were exposed to control (*C*) medium or conditioned medium from H157S2 cells (*S*) and immunoblots were done as in *A*. Actin was used as a loading control. *Arrows,* signaling changes with SEMA3F.

SEMA3F expression is directed by a tetracycline/doxycycline-inducible promoter (inducible H157; Fig. 1*B*). This approach eliminates clonal selection. SEMA3F induction following doxycycline treatment was verified at the protein level (Supplementary Fig. S1*B*). In agreement, after induction of SEMA3F with doxycycline, decreases in AKT and STAT3 phosphorylation were evident (Fig. 1*B*). Next, we screened a panel of eight lung cancer cell lines, including H157, to estimate the frequency of SEMA3F-responsive cell lines (Fig. 1*C*). Cells were exposed to control or SEMA3F-conditioned medium and signaling changes were analyzed by immunoblot. Among the pathways studied, ERK1/2 was found to be the most sensitive marker with four of eight cell lines responding. It is possible that transfection with *SEMA3F* would result in a higher frequency of STAT3 and AKT responses. We concluded that responses to SEMA3F are frequent among lung cancer cell lines and that phospho-ERK1/2 inhibition is the most sensitive biochemical indicator with the use of cultured supernatants.

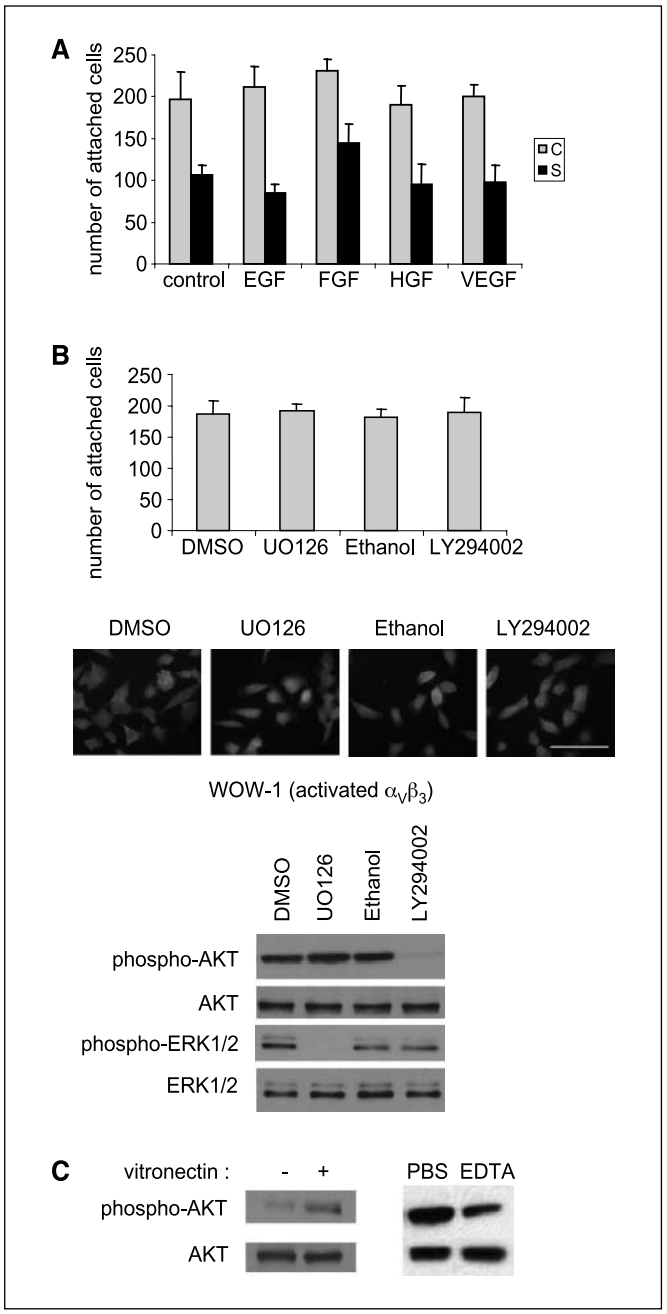

Figure 2. SEMA3F reduces adhesion to vitronectin. *A,* adhesion assay to vitronectin of untransfected H157 cells resuspended in control medium (*C*) or SEMA3F-containing medium (*S*) with 100 ng/mL of different growth factors. Cells were allowed to attach for 1 h before microscopic counting. Assays were done twice in triplicate. *Bars,* SD. *B, top,* untransfected H157 cells were resuspended in fresh medium and their ability to adhere during 1 h to vitronectin was tested in the presence of UO126 or LY294002 at 10 μmol/L and controls DMSO or ethanol. Assays were done twice in triplicate. *Bars,* SD. *Middle,* H157 cells were treated for 1 h with 10 μmol/L UO126 or LY294002 and immunofluorescence with WOW-1 antibody shows similar activation of $\alpha_v\beta_3$ integrin. Bar, 100 μm. *Bottom,* immunoblots anti–phospho-Ser^{473}-AKT and total AKT and phospho-Thr^{202}/Tyr^{204}-ERK1/2 and total ERK1/2 show the specificity and efficiency of the inhibitors. *C, left,* parental H157 cells were detached using PBS with 0.1% EDTA, rinsed in fresh medium, and plated for 2 h on bovine serum albumin–treated wells coated with (+) or without (−) vitronectin. Recovery of phospho-Ser^{473}-AKT was examined by immunoblot with total AKT as loading control. *Right,* untransfected H157 cells in culture were rapidly rinsed with PBS and divalent cation-dependent membrane proteins were inactivated for 1 min with Ca^{2+}/Mg^{2+}-free PBS containing 0.1% EDTA. Cells were incubated for 15 min in their own medium and lysed and phospho-Ser^{473}-AKT and total AKT were monitored by immunoblot.

Possible involvement of integrin outside-in signaling in SEMA3F effects. Beyond its effects on ERK1/2 phosphorylation, expression of SEMA3F leads to the loss of activated $\alpha_v\beta_3$ staining in H157 cells and reduced adhesion to ECM (6). Indeed, exposure of H157 cells to SEMA3F-conditioned medium reduced adhesion to vitronectin, and interestingly, growth factors stimulation did not rescue this inhibitory effect (Fig. 2*A*). We therefore explored the relationship between adhesion and the signaling effect of SEMA3F. We first asked whether AKT or ERK1/2 inactivation by specific inhibitors (LY294002 and UO126, respectively) would mimic the SEMA3F effect on activated $\alpha_v\beta_3$ integrin or adhesion to vitronectin. As shown in Fig. 2*B*, neither inhibitor affected $\alpha_v\beta_3$ activation (as determined with WOW-1 staining) or adhesion, although the drugs did inhibit their respective targets. Thus, AKT and ERK1/2 do not inhibit adhesion by inside-out signaling. On the other hand, adhesion inhibition by SEMA3F could mediate loss of phospho-ERK1/2 and phospho-AKT by outside-in signaling. Accordingly, brief treatment of H157 cells with EDTA to dissociate their membrane contacts resulted in down-regulation of phospho-AKT, and plating cells on vitronectin after cell detachment increased AKT activation (Fig. 2*C*). These results support the hypothesis that SEMA3F impairs the maintenance of active signaling pathways by inhibiting integrin-mediated outside-in signaling.

ILK inhibition by SEMA3F leads to phospho-ERK1/2 loss. Integrins connect various protein kinases, including ILK, which mediate intracellular signaling. To determine if ILK activity was affected by SEMA3F, we immunoprecipitated ILK from control (H157C) or SEMA3F (H157S2) cells. As shown in the silver-stained gel and total ILK immunoblot in Fig. 3*A*, equal amounts of ILK were precipitated. We found that ILK activity, as determined by an *in vitro* kinase assay using MBP as substrate, was reduced in H157S2 cells by 55% (Fig. 3*A, right*). This finding was specific because phospho-FAK (Tyr^{397}) was unchanged (data not shown). ILK activation has been shown to induce AKT phosphorylation on residue Ser^{473} (22), and ILK inhibition, at least in some cellular contexts, leads to down-regulation of phospho-STAT3 over time (23). Thus, we asked if ILK inhibition could account for the signaling changes observed with SEMA3F. Surprisingly, we found that ILK inhibition by siRNA in H157 cells caused loss of phospho-ERK1/2 after 72 h but not phospho-AKT (Fig. 3*B*). Moreover, STAT3 was unexpectedly activated probably due to increased total levels. These results suggested that other integrin-associated proteins control AKT-STAT3 in H157 cells. Accordingly, inhibition of Src family kinases by PP2 lowered AKT phosphorylation, and phospho-STAT3 was slightly affected (Fig. 3*C*). Together, these data indicate that ILK is a link between SEMA3F effects on adhesion and ERK1/2 signaling, and preliminary data suggest that the effects on AKT-STAT3 result from a Src family kinase inhibition.

Repercussion of AKT pathway inhibition by SEMA3F on HIF-1α/VEGF. HIF-1α is regulated at the level of protein initiation by activation of AKT and its downstream effector mammalian target of rapamycin (mTOR; ref. 24). HIF-1α protein levels are also regulated by von Hippel-Lindau (VHL)-mediated polyubiquitination and subsequent proteasome-dependent degradation (25). At the transcriptional level, both HIF and phospho-STAT3 regulate VEGF-A mRNA levels (26). Based on the above results, we compared HIF-1α and VEGF levels in SEMA3F-expressing H157 cells and controls. HIF-1α protein levels were reduced in SEMA3F-expressing clones both in normoxia and severe hypoxia (0.01% O_2; Fig. 4*A, left*). This loss was further confirmed by exposure of parental H157 cells to SEMA3F-conditioned medium (data not shown). By immunofluorescence (Fig. 4*A, right*), nuclear HIF-1α protein levels were markedly diminished in SEMA3F-expressing clones, in normoxia, and in response to the severe hypoxia mimetic

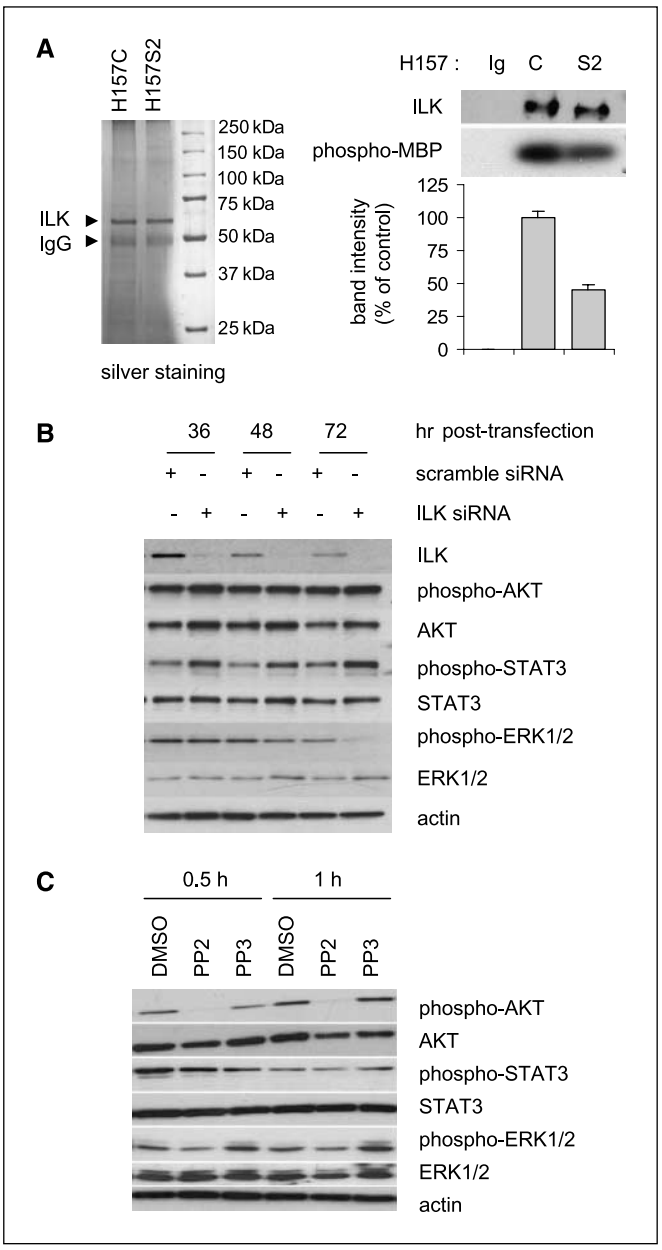

Figure 3. SEMA3F reduces ILK activity. *A, left,* silver staining of ILK immunoprecipitate showing the purity of the preparation from H157C and H157S2 cells used for kinase activity assay. *Top right,* immunoblot showing precipitated ILK and ILK activity. Kinase assay was carried out on MBP in the presence of ATP and phospho-MBP was detected by immunoblot anti–phospho-serine/threonine. *Lane Ig,* control immunoprecipitation with unrelated IgG, which was used to confirm the absence of autophosphorylation of MBP. *Bottom right,* absorbance of the phospho-MBP bands was determined by CCD camera scan (Biocom Visio). *Bars,* SD. *B,* parental H157 cells were transfected with control scramble or ILK siRNA and effects on signaling were monitored over time by immunoblot for ILK, phospho-Ser^{473}-AKT and total AKT, phospho-Tyr^{705}-STAT3 and total STAT3, and phospho-Thr^{202}/Tyr^{204}-ERK1/2 and total ERK1/2. *C,* parental H157 cells were treated with the Src inhibitor PP2 at 20 μmol/L for 30 min or 1 h, its control ineffective analogue PP3, or equivalent volume of DMSO, and effects on signaling were monitored over time by immunoblot for phospho-Ser^{473}-AKT and total AKT, phospho-Tyr^{705}-STAT3 and total STAT3, and phospho-Thr^{202}/Tyr^{204}-ERK1/2 and total ERK1/2. Actin was used as a loading control.

$CoCl_2$. To determine the mechanisms underlying HIF-1α loss, we examined HIF-1α transcript levels by real-time RT-PCR and found them unchanged (Fig. 4*B, left*). To examine HIF-1α protein stability, cells were first treated with the proteasome inhibitor MG132 to allow HIF-1α accumulation and then washed and treated with cycloheximide to inhibit new protein synthesis. As shown in Fig. 4*B*, HIF-1α levels disappeared at approximately the same rate in control and SEMA3F-expressing cells (S2). We also transfected H157C and S2 clones with a HIF-1α mutant insensitive to VHL-dependent degradation and found that SEMA3F-expressing cells had substantially lower levels than control cells (data not shown). Therefore, the reduction of HIF-1α in H157 cells by SEMA3F is not the result of impaired transcription or enhanced degradation. Thus, it is likely that HIF-1α protein translation, which is promoted by AKT-mTOR (24), is reduced by SEMA3F. Consistently, inhibition of AKT with LY294002 also led to loss of HIF-1α (Fig. 4*C, left*). We examined HIF-1α protein levels in three other *SEMA3F* stably transfected cell lines from different origin (Fig. 4*C, right*). HIF-1α level was reduced in all SEMA3F-expressing cell lines except the MCF7 mammary adenocarcinoma cells in which it was increased; the reason of which is unknown. Furthermore, $CoCl_2$ treatment markedly induced HIF-1α in control cells but only weakly in SEMA3F-H460 and SEMA3F-COS7 cells. Based on these results, we conclude that SEMA3F down-regulates HIF-1α through inhibition of AKT and protein translation.

In agreement with the effects on HIF-1α, we found that both VEGF mRNA and protein levels were significantly reduced in the SEMA3F-expressing H157 and H460 cells (Fig. 4*D*). The same result was obtained with *SEMA3F*-transfected COS7 cells (VEGF mRNA reduced by 74%; Supplementary Table S1). In contrast, a modest increase of VEGF mRNA was seen in MCF7 (+18% of controls; Supplementary Table S1).

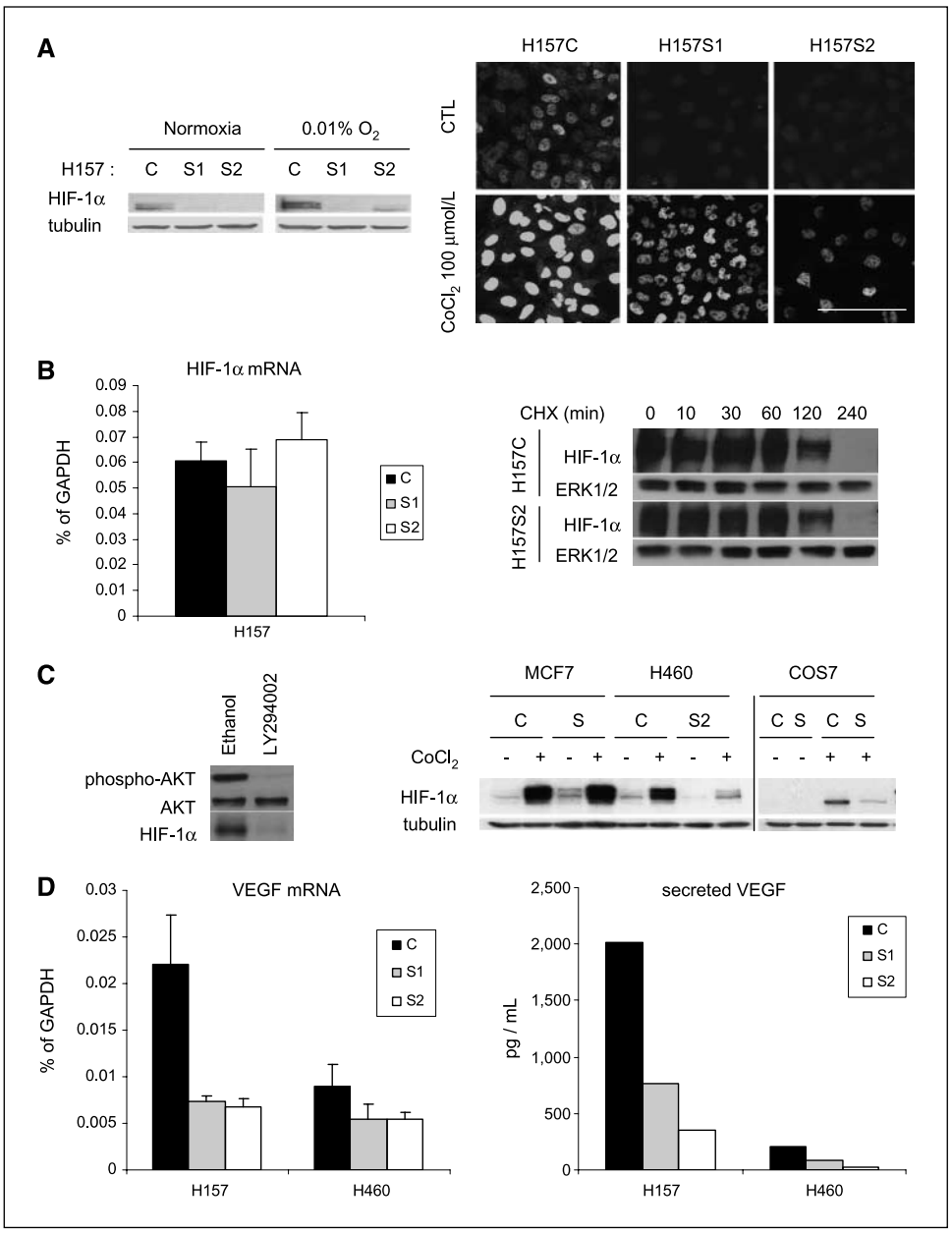

Figure 4. SEMA3F down-regulates HIF-1α protein and VEGF mRNA. *A, left,* HIF-1α protein expression by immunoblot in H157C and H157S1/S2 exposed for 6 h to normoxia or severe hypoxia (0.01% O_2). Tubulin shows protein loading control. *Right,* immunostaining with anti-HIF-1α antibody was done on control and SEMA3F-H157 cells grown 6 h in the presence or absence of 100 μmol/L $CoCl_2$. Bar, 100 μm. *B, left,* HIF-1α mRNA levels in H157C, H157S1, and H157S2 clones were measured by quantitative real-time RT-PCR. Values are expressed as % of GAPDH. Determinations were done twice in duplicate. *Bars,* SD. *Right,* HIF-1α half-life in H157C and H157S2 clones. Both clones were treated with 10 μmol/L of the proteasome inhibitor MG132 for 6 h to increase HIF-1α levels for purposes of detection in H157S2 cells. After withdrawal of MG132, protein synthesis inhibitor cycloheximide (*CHX*) was added at 100 pg/mL and HIF-1α was monitored by immunoblot over time. ERK1/2 is shown as loading control. The H157S2 HIF-1α immunoblot was overexposed about four times to give signal intensity similar to that of H157C. *C, left,* parental H157 cells were treated for 6 h with ethanol or 10 μmol/L LY294002, and effects on signaling were monitored by immunoblot for phospho-Ser^{473}-AKT, total AKT, and HIF-1α. *Right,* control or SEMA3F cells were treated for 3 h in the presence or absence of 100 μmol/L $CoCl_2$. *C,* control cells; *S, SEMA3F* stably transfected polyclonal population; *S2, SEMA3F* stably transfected clone 2. Following treatment, cells were lysed and HIF-1α was monitored by immunoblot with tubulin as loading control. *D, left,* $VEGF_{165}$ mRNA levels in control clones (H157C) and *SEMA3F*-transfected clones were measured by quantitative real-time RT-PCR and expressed in % of GAPDH. The experiments were done five times in duplicate. *Bars,* SD. *Right,* $VEGF_{165}$ protein levels from culture medium of control H157 and H157S1/S2 were measured by ELISA. Measurements were done in quadruplicate.

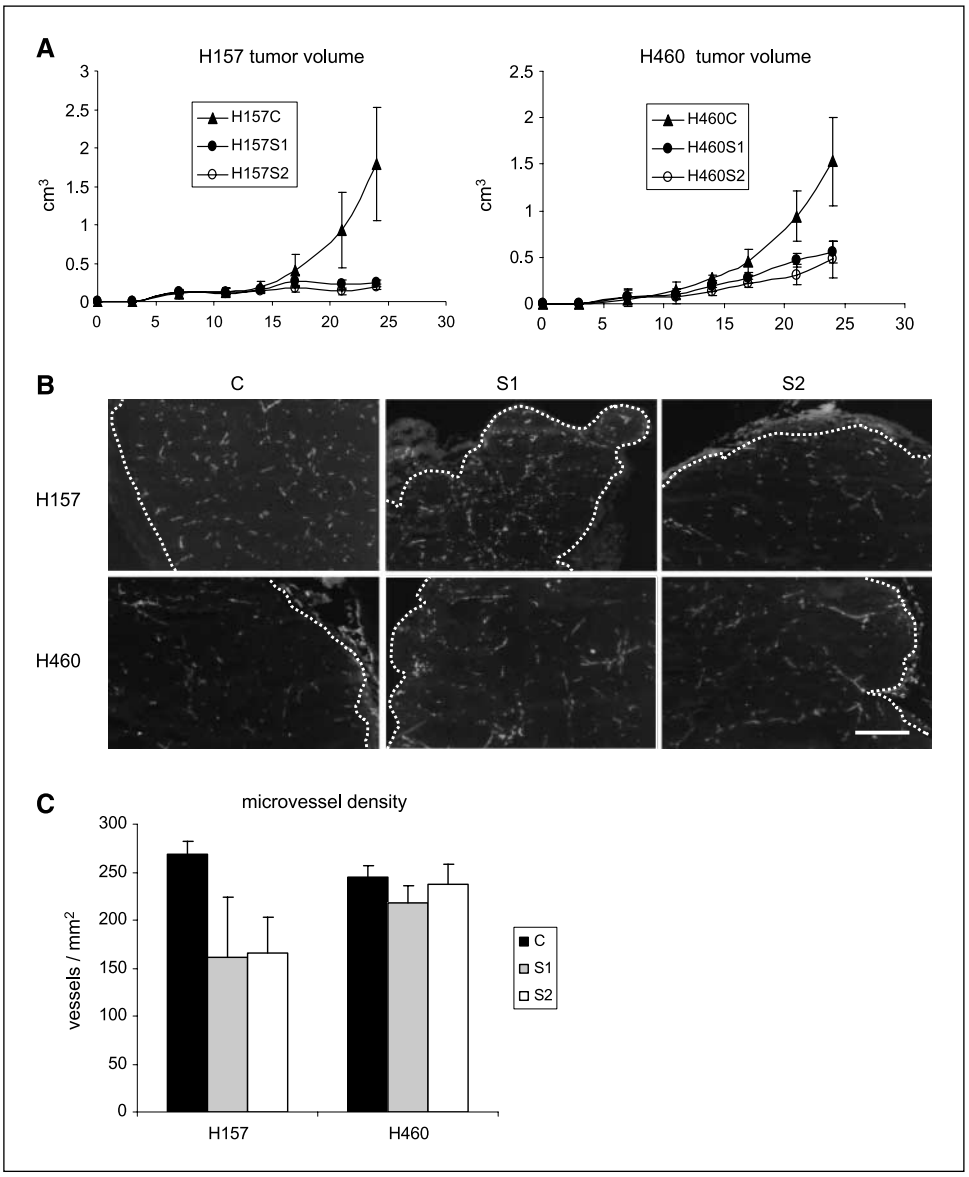

Figure 5. SEMA3F-expressing H157 cells form small tumors *in vivo* with reduced vascularization. *A,* H157 or H460 tumor cells suspended in Matrigel were injected s.c. in NMRI-*nu/nu* mice (five animals per group). Tumor volumes were measured every 3 d after inoculation. *Bars,* SD. *B,* cryosections done on H157- or H460-derived tumors were immunostained for CD31. Bar, 500 μm. *C,* quantification of microvessel density in H157- and H460-derived tumors. Counting was done within three random areas of three sections of each tumor. *Bars,* SE.

Inhibition of tumor growth by SEMA3F. VEGF is a well-established master regulator of angiogenesis *in vivo*. We consequently questioned whether SEMA3F up-regulation would interfere with tumor angiogenesis and tumor growth. A Matrigel suspension of H157 control or SEMA3F-expressing cells was injected s.c. into the right flanks of nude mice. Interestingly, there was no apparent inhibition of tumor growth by SEMA3F until day 14 (Fig. 5*A*). By day 24, however, tumor volumes (Fig. 5*A*) and microvessel density (Fig. 5*B* and *C*), as determined by CD31 (platelet/endothelial cell adhesion molecule-1) immunostaining, were significantly reduced by SEMA3F expression. H157S1- and H157S2-induced tumors had an average volume of 0.2 cm^3, whereas control tumors had grown to 1.8 ± 0.3 cm^3. Correspondingly, tumor weights were decreased by ~94% (data not shown).

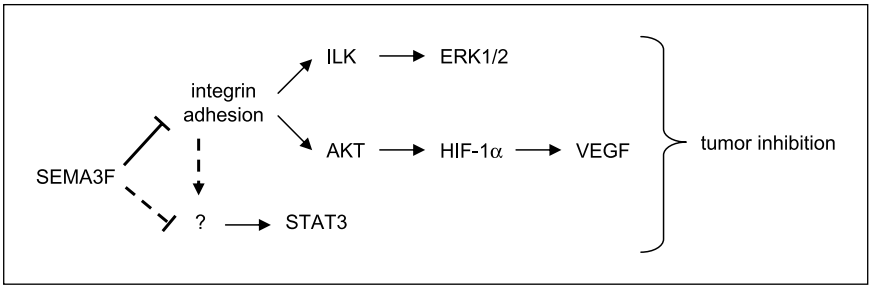

Figure 6. A theoretical model for SEMA3F tumor inhibition.

Blood vessels were more homogeneously distributed in tumors derived from H157C compared with H157S1 and H157S2 tumors. Likewise, the vessels were also strikingly smaller in the SEMA3F-H157–induced tumors. Interestingly, SEMA3F also prevented development of H460-derived tumors, although the vascularization was not significantly different and the suppressive effect on tumor growth was not as dramatic as with H157 cells. These results indicate that angiogenesis inhibition by SEMA3F only partially contributes to the tumor prevention and that additional effects, such as signaling inhibition, might play an independent role.

Discussion

The reexpression of SEMA3F in cancer cells was previously shown to impair *in vivo* tumorigenicity in three different s.c. models (27–29). More recently, using a lung orthotopic model, we reported that SEMA3F blocked H157 lung cancer cell-derived tumorigenesis and suggested that down-regulation of active $\alpha_v\beta_3$ integrin and phospho-ERK1/2 could explain this effect (6). In the present report, we have shown that ILK activity is down-regulated in *SEMA3F*-transfected H157 cells, and inhibition of ILK leads to reduced phospho-ERK1/2. In parallel, SEMA3F reexpression caused reduction in phospho-AKT (Ser^{473}) and phospho-STAT3 (Tyr^{705}), with downstream effects on HIF-1α and VEGF (see speculative model in Fig. 6). In contrast to phospho-ERK1/2, phospho-STAT3 and phospho-AKT were not inhibited by a knockdown of ILK. The AKT and STAT3 effects are likely mediated by a Src family kinase, which are known to constitutively associate with β-integrin tails. To our knowledge, this is the first report describing inhibition of ILK, STAT3, and HIF by semaphorins. Importantly, the effects of SEMA3F were not limited to H157 cells. Using transferred cultured supernatants, ERK1/2 inactivation by SEMA3F was found in four of eight lung cancer cell lines. In addition, HIF-1α and VEGF reduction were observed in three of four cell lines of different origins stably transfected with *SEMA3F*.

Recently, Ito et al. (30) reported that Sema4D suppressed R-Ras activity along with dephosphorylation of AKT in hippocampal neurons. This relationship was subsequently strengthened by evidence that R-Ras is upstream of ILK and glycogen synthase kinase-3β in this system (31). In addition, SEMA3A inhibited phospho-AKT in dorsal root ganglia growth cones and breast cancer cell lines through wild-type phosphatase and tensin homologue (PTEN; ref. 32). However, H157 cells have a mutant *PTEN* gene (33), which we confirmed by DNA sequence analysis and the absence of PTEN protein (Supplementary Fig. S1*C*). In addition, Ser^{473} of AKT has been directly shown to be a target of ILK (34–36), requiring $\alpha_v\beta_3$ integrin function that is independent of PTEN (35). Thus, PTEN is dispensable for SEMA3F signaling in some cellular contexts.

We found that HIF-1α is inhibited by SEMA3F at the level of protein translation initiation in H157 cells, with corresponding effects on VEGF mRNA and protein. Similar decreases in HIF-1α and VEGF were observed in additional (two of three) cell lines. This likely results from AKT inactivation by SEMA3F because inhibiting AKT with LY294002 induced loss of HIF-1α. In agreement, Vacca et al. (37) reported that SEMA3A reduced VEGF mRNA levels in endothelial cells isolated from patients with multiple myeloma, although the mechanism was not explored. Of interest, VEGF transcription is also regulated by a STAT3 binding site in the VEGF promoter (26), with an important contribution of Tyr^{705} STAT3 phosphorylation (38). Thus, SEMA3F-mediated inhibition of VEGF mRNA probably involves both HIF and STAT3 effects. Accordingly, both microvessel density and size were reduced in s.c. tumors induced by SEMA3F-H157 cells compared with control cells. Tumor size was also reduced after an initial period of indistinguishable growth, consistent with an angiogenic effect. Although VEGF may be one of the most important angiogenic factors affected by SEMA3F, our preliminary data indicate that other angiogenic mediators are also involved (data not shown).

Lastly, because SEMA3F inhibits several signaling components, it is tempting to hypothesize that up-regulation of SEMA3F would be more effective than an ILK, AKT, or ERK1/2 inhibition alone, although combined inhibitors may recapitulate the effects of SEMA3F. To up-regulate endogenous SEMA3F expression in tumor cells, only nonspecific histone deacetylase inhibitors can be presently used for this purpose (39); thus, further studies to understand *SEMA3F* gene regulation are necessary.

Acknowledgments

Received 9/28/2006; revised 5/30/2007; accepted 6/29/2007.

Grant support: University of Colorado Lung Cancer Specialized Program of Research Excellence grant CA58187 (R.M. Gemmill and H.A. Drabkin), La Ligue Contre le Cancer (V. Potiron, J.A. Clarhaut, and J. Roche), l'Association pour la Recherche sur le Cancer (V. Potiron, J.A Clarhaut, and J. Roche), Alexander Von Humboldt Foundation (P. Nasarre), and Deutsche Forschungsgemeinschaft SPP1190 Au83/9-1 (H.G. Augustin).

The costs of publication of this article were defrayed in part by the payment of page charges. This article must therefore be hereby marked *advertisement* in accordance with 18 U.S.C. Section 1734 solely to indicate this fact.

References

1. Roche J, Boldog F, Robinson M, et al. Distinct 3p21.3 deletions in lung cancer and identification of a new human semaphorin. Oncogene 1996;12:1289–97.
2. Sekido Y, Bader S, Latif F, et al. Human semaphorins A(V) and IV reside in the 3p21.3 small cell lung cancer deletion region and demonstrate distinct expression patterns. Proc Natl Acad Sci U S A 1996;93:4120–5.
3. Xiang RH, Hensel CH, Garcia DK, et al. Isolation of the human semaphorin III/F gene (SEMA3F) at chromosome 3p21, a region deleted in lung cancer. Genomics 1996;32:39–48.
4. Brambilla E, Constantin B, Drabkin H, Roche J. Semaphorin SEMA3F localization in malignant human lung and cell lines: a suggested role in cell adhesion and cell migration. Am J Pathol 2000;156:939–50.
5. Lantuejoul S, Constantin B, Drabkin H, Brambilla C, Roche J, Brambilla E. Expression of VEGF, semaphorin SEMA3F, and their common receptors neuropilins NP1 and NP2 in preinvasive bronchial lesions, lung tumours, and cell lines. J Pathol 2003;200:336–47.
6. Kusy S, Nasarre P, Chan D, et al. Selective suppression of *in vivo* tumorigenicity by semaphorin SEMA3F in lung cancer cells. Neoplasia 2005;7:457–65.
7. Luo Y, Raible D, Raper JA. Collapsin: a protein in brain that induces the collapse and paralysis of neuronal growth cones. Cell 1993;75:217–27.
8. Potiron V, Roche J. Class 3 semaphorin signaling: the end of a dogma. Sci STKE 2005;2005:pe24.
9. Soker S, Takashima S, Miao HQ, Neufeld G, Klagsbrun M. Neuropilin-1 is expressed by endothelial and tumor cells as an isoform-specific receptor for vascular endothelial growth factor. Cell 1998;92:735–45.
10. Migdal M, Huppertz B, Tessler S, et al. Neuropilin-1 is a placenta growth factor-2 receptor. J Biol Chem 1998;273:22272–8.
11. Miao HQ, Soker S, Feiner L, Alonso JL, Raper JA, Klagsbrun M. Neuropilin-1 mediates collapsin-1/semaphorin III inhibition of endothelial cell motility: functional competition of collapsin-1 and vascular endothelial growth factor-165. J Cell Biol 1999;146:233–42.
12. Castro-Rivera E, Ran S, Thorpe P, Minna JD. Semaphorin 3B (SEMA3B) induces apoptosis in lung and breast cancer, whereas VEGF165 antagonizes this effect. Proc Natl Acad Sci U S A 2004;101:11432–7.
13. Jin Z, Strittmatter SM. Rac1 mediates collapsin-1-induced growth cone collapse. J Neurosci 1997;17:6256–63.
14. Toyofuku T, Yoshida J, Sugimoto T, et al. FARP2 triggers signals for Sema3A-mediated axonal repulsion. Nat Neurosci 2005;8:1712–9.
15. Serini G, Valdembri D, Zanivan S, et al. Class 3 semaphorins control vascular morphogenesis by inhibiting integrin function. Nature 2003;424:391–7.
16. Banu N, Teichman J, Dunlap-Brown M, Villegas G,

Tufro A. Semaphorin 3C regulates endothelial cell function by increasing integrin activity. FASEB J 2006; 20:2150–2.
17. Oinuma I, Ishikawa Y, Katoh H, Negishi M. The semaphorin 4D receptor plexin-B1 is a GTPase activating protein for R-Ras. Science 2004;305:862–5.
18. Oinuma I, Katoh H, Negishi M. Semaphorin 4D/plexin-B1-mediated R-Ras GAP activity inhibits cell migration by regulating β1 integrin activity. J Cell Biol 2006;173:601–13.
19. Ginsberg MH, Partridge A, Shattil SJ. Integrin regulation. Curr Opin Cell Biol 2005;17:509–16.
20. Hannigan GE, Leung-Hagesteijn C, Fitz-Gibbon L, et al. Regulation of cell adhesion and anchorage-dependent growth by a new β1-integrin-linked protein kinase. Nature 1996;379:91–6.
21. Hannigan G, Troussard AA, Dedhar S. Integrin-linked kinase: a cancer therapeutic target unique among its ILK. Nat Rev Cancer 2005;5:51–63.
22. Troussard AA, Mawji NM, Ong C, Mui A, St.-Arnaud R, Dedhar S. Conditional knock-out of integrin-linked kinase demonstrates an essential role in protein kinase B/Akt activation. J Biol Chem 2003;278:22374–8.
23. Yau CY, Wheeler JJ, Sutton KL, Hedley DW. Inhibition of integrin-linked kinase by a selective small molecule inhibitor, QLT0254, inhibits the PI3K/PKB/mTOR, Stat3, and FKHR pathways and tumor growth, and enhances gemcitabine-induced apoptosis in human orthotopic primary pancreatic cancer xenografts. Cancer Res 2005; 65:1497–504.
24. Phillips RJ, Mestas J, Gharaee-Kermani M, et al. Epidermal growth factor and hypoxia-induced expression of CXC chemokine receptor 4 on non-small cell lung cancer cells is regulated by the phosphatidylinositol 3-kinase/PTEN/AKT/mammalian target of rapamycin signaling pathway and activation of hypoxia inducible factor-1α. J Biol Chem 2005;280: 22473–81.
25. Cockman ME, Masson N, Mole DR, et al. Hypoxia inducible factor-α binding and ubiquitylation by the von Hippel-Lindau tumor suppressor protein. J Biol Chem 2000;275:25733–41.
26. Gray MJ, Zhang J, Ellis LM, et al. HIF-1α, STAT3, CBP/p300 and Ref-1/APE are components of a transcriptional complex that regulates Src-dependent hypoxia-induced expression of VEGF in pancreatic and prostate carcinomas. Oncogene 2005;24:3110–20.
27. Xiang R, Davalos AR, Hensel CH, Zhou XJ, Tse C, Naylor SL. Semaphorin 3F gene from human 3p21.3 suppresses tumor formation in nude mice. Cancer Res 2002;62:2637–43.
28. Kessler O, Shraga-Heled N, Lange T, et al. Semaphorin-3F is an inhibitor of tumor angiogenesis. Cancer Res 2004;64:1008–15.
29. Bielenberg DR, Hida Y, Shimizu A, et al. Semaphorin 3F, a chemorepulsant for endothelial cells, induces a poorly vascularized, encapsulated, nonmetastatic tumor phenotype. J Clin Invest 2004;114:1260–71.
30. Ito Y, Oinuma I, Katoh H, Kaibuchi K, Negishi M. Sema4D/plexin-B1 activates GSK-3β through R-Ras GAP activity, inducing growth cone collapse. EMBO Rep 2006; 7:704–9.
31. Oinuma I, Kato H, Negishi M. R-Ras controls axon specification upstream of glycogen synthase kinase-3β through integrin-linked kinase. J Biol Chem 2007;282: 303–18.
32. Chadborn NH, Ahmed AI, Holt MR, et al. PTEN couples Sema3A signalling to growth cone collapse. J Cell Sci 2006;119:951–7.
33. Forgacs E, Biesterveld EJ, Sekido Y, et al. Mutation analysis of the PTEN/MMAC1 gene in lung cancer. Oncogene 1998;17:1557–65.
34. Delcommenne M, Tan C, Gray V, Rue L, Woodgett J, Dedhar S. Phosphoinositide-3-OH kinase-dependent regulation of glycogen synthase kinase 3 and protein kinase B/AKT by the integrin-linked kinase. Proc Natl Acad Sci U S A 1998;95:11211–6.
35. Cruet-Hennequart S, Maubant S, Luis J, Gauduchon P, Staedel C, Dedhar S. α(v) integrins regulate cell proliferation through integrin-linked kinase (ILK) in ovarian cancer cells. Oncogene 2003;22:1688–702.
36. Tan C, Cruet-Hennequart S, Troussard A, et al. Regulation of tumor angiogenesis by integrin-linked kinase (ILK). Cancer Cell 2004;5:79–90.
37. Vacca A, Scavelli C, Serini G, et al. Loss of inhibitory semaphorin 3A (SEMA3A) autocrine loops in bone marrow endothelial cells of patients with multiple myeloma. Blood 2006;108:1661–7.
38. Schaefer LK, Wang S, Schaefer TS. c-Src activates the DNA binding and transcriptional activity of Stat3 molecules: serine 727 is not required for transcriptional activation under certain circumstances. Biochem Biophys Res Commun 1999;266:481–7.
39. Kusy S, Potiron V, Zeng C, et al. Promoter characterization of semaphorin SEMA3F, a tumor suppressor gene. Biochim Biophys Acta 2005;1730:66–76.

Semaphorin SEMA3F Affects Multiple Signaling Pathways in Lung Cancer Cells

Vincent A. Potiron, Girish Sharma, Patrick Nasarre, et al.

Cancer Res 2007;67:8708-8715.